Chemometrics and Intelligent Laboratory Systems 113 (2012) 58–67

Contents lists available at SciVerse ScienceDirect

Chemometrics and Intelligent Laboratory Systems

journal homepage: www.elsevier.com/locate/chemolab

Application of 2D correlation spectroscopy on olive stones acid hydrolysates: Effect of overliming

Jeanne Andary [a,*], Jacqueline Maalouly [c], Rosette Ouaini [c], Hanna Chebib [c], Douglas N. Rutledge [a,d], Naim Ouaini [b]

[a] AgroParisTech, Laboratoire de Chimie Analytique, 16 rue Claude Bernard, 75005 Paris, France
[b] URA (CNRS/USEK/UL) GREVE, Departement of Chemistry and Life Science, Université Saint-Esprit de Kaslik, 446 Jounieh, Lebanon
[c] URA (CNRS/USEK/UL) GREVE, Departement of Chemistry, Faculty of Science, Lebanese University, 90656, Jdaideth El Maten, Fanar, Lebanon
[d] INRA/AgroParisTech UMR1145 GENIAL Ingénierie Procédés Aliments, 16, rue Claude Bernard. 75005, Paris, France

ARTICLE INFO

Article history:
Received 31 January 2011
Received in revised form 1 November 2011
Accepted 9 November 2011
Available online 25 November 2011

Keywords:
Olive stones
Dilute acid hydrolysate
Xylose
Furfural
Hydroxyl-methylfurfural
2DCOS

ABSTRACT

In order to valorize olive stones we are studying their dilute-acid hydrolysate (DAH) composition, and trying to highlight the effect of the overliming process on DAH composition in order to perform an effective treatment that maximize sugars concentrations (xylose) and minimizes the amount of toxic materials (FF and HMF). An $2^2 3^1$ experimental design was established to describe the effects of three controlled factors with distinct levels: pH (10 and 12), temperature (25 and 60 °C) and detoxification time (15, 30 and 60 min) on the concentration of xylose, FF and HMF. A better understanding of this overliming process was possible by exploring the chromatograms obtained with 2D Correlation Spectroscopy (2DCOS). 2D correlation spectroscopy gave information about the relations that exist between chromatographic peaks and chromatograms. The order in which the constituents vary can be deduced from the sign of peaks in the synchronous and asynchronous matrices, facilitating the interpretation of kinetic studies.

© 2011 Published by Elsevier B.V.

1. Introduction

Over eight million hectares of olive trees are cultivated worldwide, most of them in Mediterranean countries [1]. Agricultural residues are abundant, renewable, low cost raw materials that may be transformed into valuable products (biofuels, biofertilizers, animal feed and chemical feed-stock) [2, 3]. Olive stones are mainly subjected to biotechnological or chemical modifications in order to be transformed into animal feed. These transformations have proven to be necessary since that olive stones present low energy due to their low content in proteins and their high content of fibers [4, 5].

To obtain fermentable monomeric sugars, lignocellulosic matrices, hemicellulose and cellulose need to be hydrolyzed [6, 7]. Dilute-acid hydrolysis (DAH) has proven to be a fast and cheap method to produce sugar from lignocellulosic materials. Hemicellulose constitutes 20–35% dry weight in lignocellulosic biomass, with D-xylose as the major sugar after hydrolysis [8]. However, dilute-acid hydrolysis leads to contains toxic compounds such as furans, aliphatic acids [9], and phenolic compounds [10]. Larsson (1999), found that overliming is the most cost effective method for detoxifying wood hydrolysates [11]. The overliming process begins by adding lime to adjust the pH of the hydrolysate liquor to a high value, the liquor is usually heated at 50 or 60 °C. Even though lime hydration is a highly exothermic reaction, heating may still be required to reach the desired temperature. Once the pH and the temperature are at the target values, the solution is held at that temperature for a period of time, and then filtered to remove the gypsum precipitate formed by divalent calcium from the lime combining with sulfate in the hydrolysate [12]. Finally re-acidification of the hydrolysate to a value appropriate for fermentation completes the process. The mechanism by which overliming reduces hydrolysate toxicity is not well known [13]. A potential drawback of overliming is sugar degradation due to hydroxide catalysed degradation reactions [14].

In order to valorize olive stones we are studying their dilute-acid hydrolysate composition, and trying to highlight the effect of the overliming process on DAH composition in order to perform an effective overliming process which maximizes sugars concentrations and minimizes the amount of toxic materials.

In a previous study we applied overliming as a detoxification treatment for the olive stones hydrolysate [15]. A $2^2 3^1$ experimental design was established to describe the effect of overliming performed at three factors: pH (10 and 12), temperature (25 and 60 °C) and detoxification time (15, 30 and 60 min) [16]. According to the study, all factors are "active"; they act by reducing the concentration of xylose, furfural (FF) and 5-hydroxymethylfurfural (HMF).

* Corresponding author at: Departement of Chemistry and Life Science, Université Saint-Esprit de Kaslik, 446 Jounieh, Lebanon. Tel.: +961 9 600900.
E-mail address: jeanne_andary@hotmail.com (J. Andary).

0169-7439/$ – see front matter © 2011 Published by Elsevier B.V.
doi:10.1016/j.chemolab.2011.11.006

The objective of the present work is to explore the chromatograms obtained under these different operating conditions using 2DCOS. This tool emphasizes the information contained in these chromatograms, which may not be visible at first sight [17].

2. Materials and methods

2.1. Dilute-acid hydrolysates (DAH), preparation and detoxification

The hydrolysis of the olive stones is carried out with a sulphuric acid solution 5% (p/v). When cooled, the solid and liquid phases are separated by filtration. The DAH is than stocked at −20 °C for further analysis. The titration is carried out with 50 $g.L^{-1}$ solution of $Ca(OH)_2$ [18].

2.2. Experimental design

Overliming is carried out under different conditions: pH (10 or 12), temperature 25 or 60 °C and time (15, 30 and 60 min). An experimental design including $2^2 \times 3^1 = 12$ experiments is prepared using Nemrodw software [19]. Each experiment was repeated three times. Table 1 summarises the different overliming conditions applied to the DAH.

2.3. Analytical methods

High-performance liquid chromatography (HPLC) is used to analyze samples. D-glucose, D-xylose, mannose and galactose are analyzed using an Aminex coloumn (Thermo Electron APS-Hypersil) and a refractive index detector (RI-150 Spectra System, Thermo Finnigan). The eluent is an isocratic phase composed of acetonitrile and water (95/5: v/v) at a flow-rate of 1 $mL.min^{-1}$. Fructose is used as an internal standard.

Furfural (FF), Hydroxymethylfurfural (HMF) and sugar degradation products such as formic, acetic, lactic and levulinic acid are analyzed on a C_{18} column with a UV detector at 280 nm (UV 1000-Thermo Finnigan). The mobile phase is composed of ultra-pure water, methanol and acetic acid (80/10/3: v/v/v) with caffeine as the internal standard. The flow is programmed to allow maximum separation of constituents: 0.5 $mL.min^{-1}$ from 0 to 10 min, 1 $mL.min^{-1}$ from 10 to 11 min (hold 9 min).

3. Chemometric tools

Two-dimensional correlation spectroscopy 2DCOS has recently received keen interest in analytical chemistry because of the following advantages: i) simplification of complex spectra consisting of many overlapping peaks; ii) enhancement of spectral resolution by spreading peaks over a second dimension; iii) establishment of unambiguous assignments through analysis of correlation bands; iv) investigations of correlations between bands in two different spectroscopic signals [20].

3.1. Generalized 2D correlation spectroscopy – principle

The two-dimensional correlation theory (2DCOS) generalized by Noda et al. [21] has been successfully utilized in MIR, NIR, Raman and other spectroscopies. It is well established that this theory may be easily adapted to other analytical methods such as chromatography [22]. 2D correlation may be applied when a set of chromatograms has an intrinsic order [23]. This technique measures the correlation among the variables or chromatographic elements; it can be used to reveal new features in data that might otherwise be overlooked. The synchronous 2DCOS matrix contains information on changes which appear simultaneously, or *in phase*. When performing the 2DCOS analysis on a single set of signals (homo-2DCOS), the peaks on the diagonal are called “auto-peaks”, while those on either side of the diagonal are “cross-peaks”. Auto-peaks are always positive because they are correlated perfectly with themselves. Cross-peaks show the existence of a relation between chromatographic peaks. In the synchronous matrix, the auto-correlation (between the same data set) is symmetrical to the diagonal because the correlation between two variables is symmetrical, whereas hetero-correlation does not present auto-peaks. A cross-peak is positive when the variations take place in the same direction, i.e. when the intensities of peaks decrease or increase at the same time; it is negative when the variations take place in opposite directions. The asynchronous matrix highlights information concerning covariations which do not occur simultaneously or at the same rate, that is are *out of phase*. The synchronous and asynchronous matrices provide complementary information. The presence of a peak in the synchronous matrix and its absence in the asynchronous matrix indicates that the peaks are perfectly correlated or *in phase* (the coefficient of correlation is then −1 or +1). The presence of an asynchronous peak at a retention time and its absence in the synchronous matrix means that the peaks variations are completely out of phase and that the correlation coefficient is then equal to zero [24]. It is also possible to probe the specific order of the chromatographic changes taking the measurement or the value of the controlling variables affecting peak orders [25]. The signs of the peaks appearing in the synchronous and asynchronous matrix are indicators of the order of appearance of the peaks [23], and can give new information on kinetics study of a process [26]. If both the synchronous and asynchronous components are positive, the feature associated with the *x*-axis leads the feature associated with the *y*-axis. However they must be changing at the same frequency to generate a correlation. If the asynchronous feature is negative, the feature associated with the *x*-axis lags the one associated with the *y*-axis. If the

Table 1
Xylose and furanes evolution according to different overliming treatments.

Treatment	pH	Temperature (°C)	Time (min)	Symbol	Xylose		FF		HMF	
					Mean	STDV	Mean	STDV	Mean	STDV
				H	10.380	0.530	51.423	0.713	10.323	0.617
1	10	25	15	A1	11.003	0.331	59.304	0.653	13.229	0.044
2			30	A2	11.172	0.240	55.974	0.659	12.100	0.922
3			60	A3	11.263	0.319	26.566	0.316	6.791	0.335
4		60	15	B1	8.415	0.061	40.097	0.579	8.711	0.650
5			30	B2	8.274	0.165	41.203	0.555	10.605	0.759
6			60	B3	7.605	0.052	30.785	0.416	7.239	0.667
7	12	25	15	C1	7.536	0.088	12.769	0.060	7.069	0.784
8			30	C2	6.068	0.060	9.894	0.856	8.045	0.829
9			60	C3	6.408	0.036	5.198	0.645	5.990	1.071
10		60	15	D1	7.373	0.048	9.247	0.135	6.710	1.075
11			30	D2	4.377	0.031	1.698	0.253	7.319	1.650
12			60	D3	2.917	0.110	2.305	0.247	7.752	0.396

synchronous feature is negative, the rules mentioned above are reversed [23].

3.2. Data matrix

Fig. 3 (A and B) shows superposed HPLC chromatograms related to DAH analysis with HPLC-UV (FF and HMF) and HPLC-RI (xylose) respectively. The starting matrix resulting from FF and the HMF chromatograms consisted of 39 samples (12*3+3 hydrolyzate) and of 12003 variables (retention time) was thus reduced to a much smaller matrix (39*3413). Matrix resulting from assembling xylose chromatograms (39*21,003) was made of 39 samples (12*3+3 hydrolyzate) and of 21,003 variables (retention time). After an ANOVA pre-treatment and while preserving interesting areas where V_G is higher than V_R, the size of the matrix becomes (39*4090).

The order of data set is arranged as shown in Table 2. Synchronous and asynchronous 2D HPLC correlation were calculated from the 39 chromatograms sets of time-resolved using CATS a statistical program developed by A.S. Barros in the analytical chemistry laboratory of the "Institut National Agronomique Paris Grignon" [27-29].

4. Results and discussion

4.1. Detoxification of the hydrolyzate

DAH detoxification effects on fermentable sugar, furfural and hydroxymethylfurfural were examined. Table 1 shows xylose and furanes evolution according to different overliming treatments. The results of detoxification are summarized in Fig. 1 (A–F). Xylose is the most abundant sugar of the hydrolysate, its average concentration being about 10.380 $g.L^{-1}$. As shown in Fig. 1A, moderate temperature at pH 10 was safe in terms of sugar loss. At 60 °C, there is a reduction in xylose concentration. When passing to pH 12, this reduction is clearer for the two temperature levels (Fig. 1B). At the end of the treatment, there remains 6.408 g.L of xylose at 25 °C and 2.917 $g.L^{-1}$ at 60 °C.

The average concentration of FF in DAH is 51.423 $mg.L^{-1}$. During liming at pH 10 this concentration decreases to 26.566 and 30.785 $mg.L^{-1}$ for 25 and 60 °C, respectively (Fig. 1C). This reduction is accentuated at pH 12. After 15 min of treatment at 25 °C the FF concentration decreases to an average value of 12.769 $mg.L^{-1}$. The most aggressive treatment leads to concentrations of 5.198 and 2.305 $mg.L^{-1}$

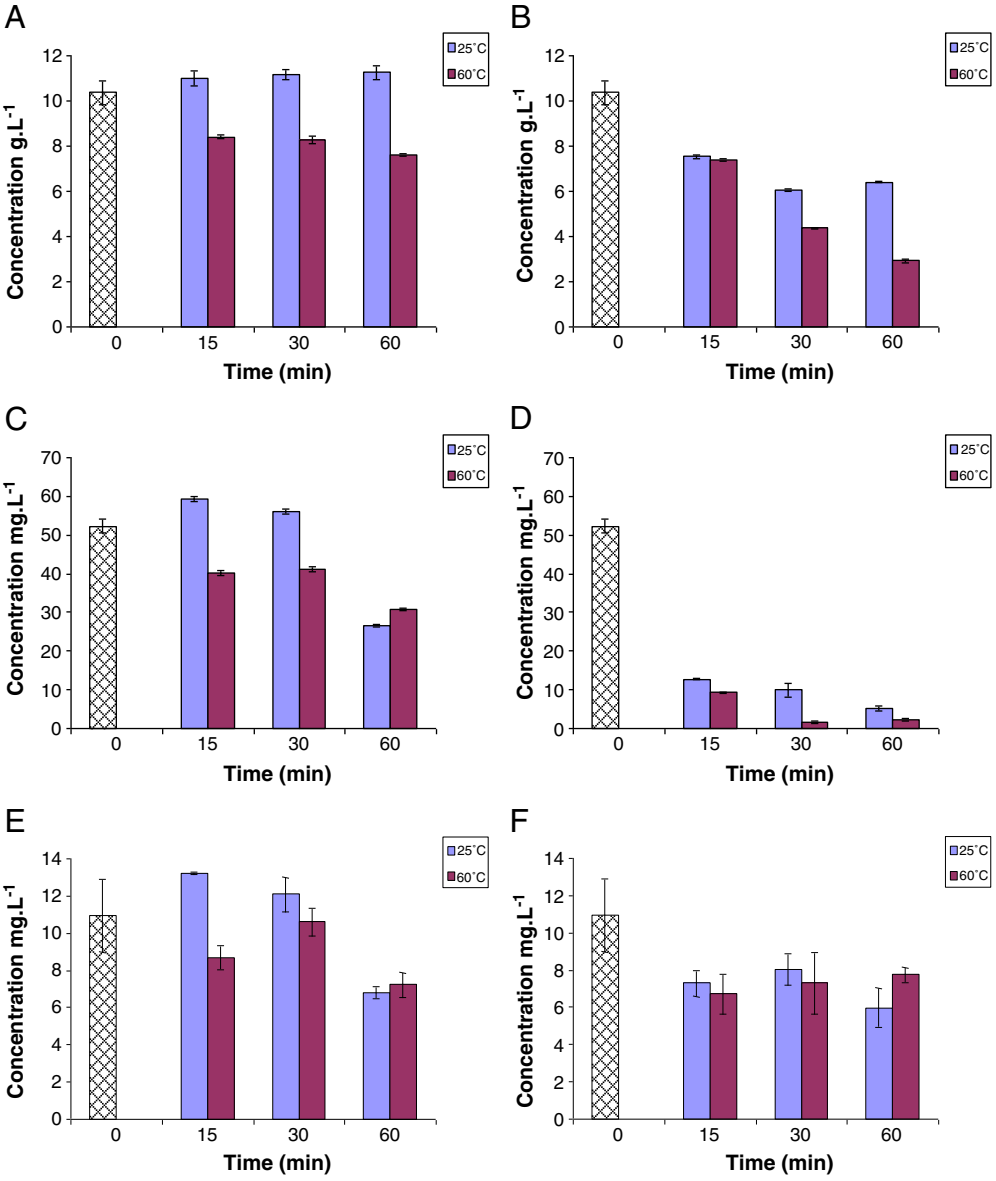

Fig. 1. Evolution of compounds during overliming process: (A) xylose pH 10, (B) xylose pH 12, (C) FF pH 10, (D) FF pH 12, (E) HMF pH 10 and (F) HMF pH 12.

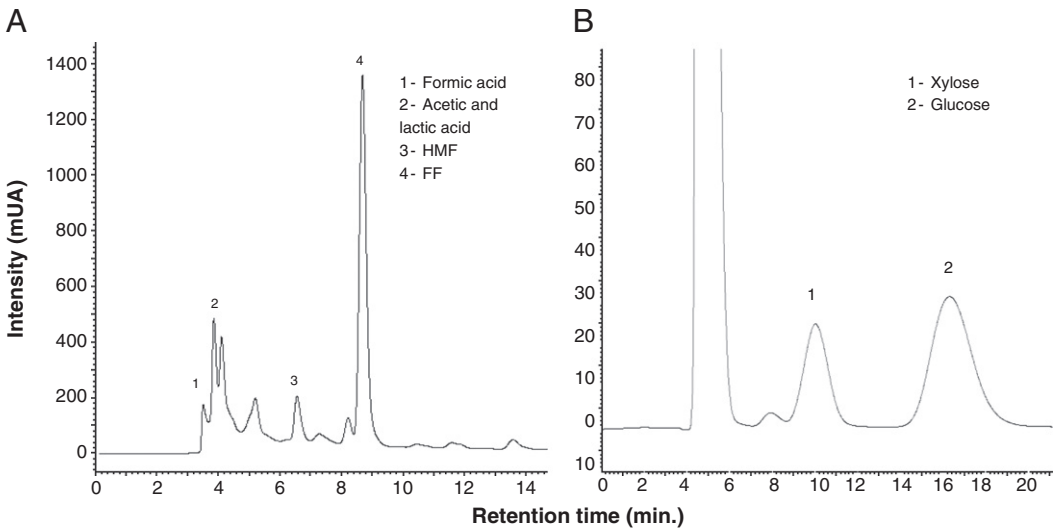

Fig. 2. Representative chromatogram for the DAH: (A) HPLC-UV, (B) HPLC-RI.

respectively at 25 and 60 °C (Fig. 1D). The initial concentration of HMF is 10.323 mg.L^{-1}, five times less than the FF concentration, probably due to the lack of hexose in the DAH. The percent decrease in HMF concentration is not as great as for xylose or FF. At the end of the detoxification process, the HMF concentration reached 7.752 mg.L^{-1} for pH 12 and 60 °C temperature, (Fig. 1E and F). These results do not directly show how overliming affects DAH components, therefore chemometric tools were applied to help in visualizing the relationships among the variables and their chronological behaviour [23].

4.2. Identification of degradation products

Fig. 2A and B shows typical HPLC-UV and HPLC-RI chromatograms for products obtained from the DAH analysis. Formic, acetic and lactic acid have been identified; however levulinic acid was not detected (Fig. 2A). We were not able to elute separately acetic and lactic acids. These results seem to be concordant with many other articles related to sugar degradation reactions [30].

Much research has been directed toward an understanding of the fundamental aspects of the alkaline degradation of saccharides. ^{13}C NMR spectroscopy has been used to study disaccharides in alkaline solution, saccharide degradation products formed via retro-aldol reactions are the salts of acids such as formic and acetic acids [31]. The main reaction of D-glucose in water at high temperature and pressures up to 80 MPa were found to be dehydratation, retro-aldol hydratation and tautomerisation reactions. Various linear compounds such as lactic, levulinic and glyceraldehydes could be obtained [32]. Yun Yan and Montgomery found that the alkaline reactions products are influenced by several parameters such as temperature, nature and the concentration of the alkali and the monosaccharide [33]. In the same study, the authors suggest that the increase of hydroxyl ion concentration and the use of divalent cations favor the formation of lactic acid and decrease the formation of C_1 (formic acid) to non lactic C_3 glyceric acid and the total amount of C_4–C_6 acid products.

However xylose, FF, HMF and aliphatic acids are not the only products formed by the dilute acid hydrolysis of olive stones. Polyphenols

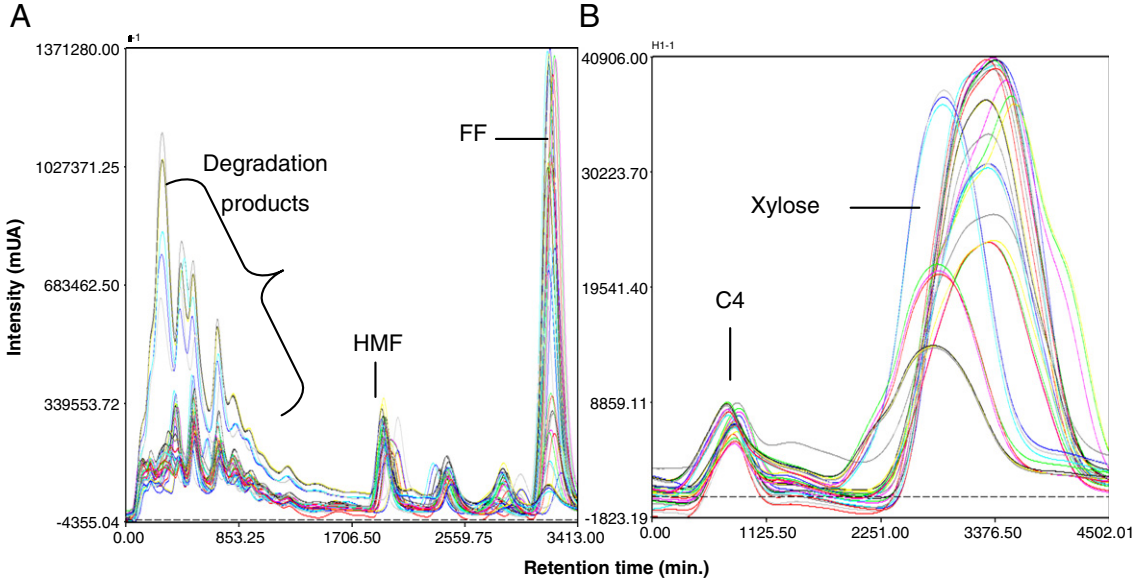

Fig. 3. Time dependent superposed chromatograms related to (A) HPLC-UV analysis and (B) HPLC-RI analysis.

Table 2
Synchronous and asynchronous correlations, signs and order of events obtained from the correlation of overlimed chromatograms.

	Correlation	Synchronous	Asynchronous	Order of events
HPLC-UV/HPLC-UV	(103 s–250 s)	−	+	250 s → 103 s
	(111 s–250 s)	−	+	250 s → 111 s
	(127 s–250 s)	−	+	250 s → 127 s
	(250 s–103 s)	−	−	250 s → 103 s
	(250 s–111 s)	−	−	250 s → 111 s
HPLC-UV/HPLC-RI	(580 s–625 s)	−	−	580 s → 625 s
	(625 s–580 s)	−		580 s → 625 s
HPLC-UV/HPLC-RI	(103 s–625 s)	−	+	625 s → 103 s
	(111 s–625 s)	−		625 s → 111 s
	(250 s–580 s)	−	−	250 s → 580 s
	(250 s–625s)	+	+	250 s → 625 s

[c]X s → Y s: the event of X occurs before that of Y

are also present in the medium and can possibly react with many hydrolysis by-products, complicating peak identification.

4.3. 2D correlation spectroscopy results

The study of the kinetics of chemical reactions is one of the useful areas for the application for the 2D correlation spectroscopy based on time dependant phenomena [23]. 2D correlation applied to high performance liquid chromatography can directly reflects the dynamic variations due to reactions occurring during the overliming process. In our study we applied 2D correlation spectroscopy to three combinations of data, first by combining chromatograms from HPLC-UV with themselves, second by combining chromatograms from HPLC-RI with themselves and finally by combining chromatograms from HPLC-UV and HPLC-RI. The application of 2DCOS to homo-chromatograms (same origin, HPLC-UV or HPLC-RI) helps identifying intra-chromatogram interactions and may help to deconvolve highly overlapped peaks by spreading them out over the second chromatogram dimension [24]. The 2DCOS hetero-chromatograms, which compare two sets of data for the same samples obtained under the same perturbation conditions with different probes, may reveal new information concerning the relations between the chromatograms [25].

4.3.1. HPLC-UV/HPLC-UV

4.3.1.1. Synchronous matrix. The synchronous matrix resulting from the homo-2D-correlation of the HPLC-UV chromatograms, consists of four regions (I, II, III and IV) (Fig. 4 A).

Region I contains two auto-peaks: (103 s–103 s), (111 s–111 s) and two cross peaks (103 s–111 s) and (111 s–103 s). Regions II and III include correlations between (103, 111, 127 s–250 s) and (250 s–103, 111, 127 s) while region IV consists of only one auto-peak (250 s -250 s). The negative signs of the cross-peaks in region III and IV mean that characteristic peak of FF appearing at ~250 s is anticorrelated with a group of peaks observed at the beginning of HPLC-UV chromatogram towards 103, 111 and 127 s [25]. Examining the chromatograms during the overliming treatments (Fig. 2) shows that the peak related to FF (~250 s) decreases with the detoxification intensity (higher pH, temperature and time), while the group of peaks observed at 103, 111, 127 s increases. The cross-peaks in region I are all positive, meaning that the set of peaks appearing at ~103, 111 and the 127 s increases with the intensity of overliming detoxification. However in the same region, we can detect correlation peaks with very weak intensity, such as: (103 s–127 s) (127 s–103 s), (111 s–127 s), (127 s–111 s), meaning that the contribution of these correlations to the reaction process must be very small [22]. A plot of the synchronous profiles related to these peaks at 103, 111, 127 and 250 s confirms that they are anticorrelated to FF (when FF decreases in concentration the set of peaks increases) (Fig. 5A and B).

4.3.1.2. Asynchronous matrix. The asynchronous matrix shown in Fig. 4 B also consists of four regions (I, II, III and IV). The absence of cross-peaks in Region I demonstrates that components at ~103 and 111 s are in perfect phase correlation. Regions III and IV show peaks at the same retention time as those of the synchronous matrix. The presence of these peaks means that FF (~250 s) and the group of peaks at ~103 and 111 s are not in perfect phase opposition. The asynchronous profiles (Fig. 5C and D) show that FF and the group of peaks at ~103 and 111 s evolve in opposite directions. The overliming process does not affect these components at the same rate; the reactions either do not occur at the same speed or do not start and stop at the same time.

4.3.2. HPLC-RI/HPLC-RI

4.3.2.1. Synchronous matrix. The synchronous matrix resulting from the homo-2DCOS of HPLC-RI chromatograms shows one large auto peak (625 s–625 s) and four cross-peaks (480 s–625 s), (625 s–480 s) and (580 s–625 s), (625 s–580 s), (Fig. 4C). The large auto peak results from the correlation of the xylose (625 s) with itself. Xylose with a concentration of 10 $g.L^{-1}$ was found to be the most abundant carbohydrate in olive stones DAH (Fig. 1A and B and Table 1). The existence of weak correlation between 480 s and 625 s reflects their limited contribution to the reaction process. However the high intensity of the negative cross-peaks (580 s–625 s) and (625 s–580 s) implies strong anticorrelation between xylose (~625 s) and the peak at ~580 s (probably a carbohydrate with four carbons). The profile relating to the two peaks at 580 s and 625 s confirms these anticorrelations (Fig. 6A and B).

4.3.2.2. Asynchronous matrix. The asynchronous matrix (Fig. 4D) shows peaks at the same retention time as those of the synchronous matrix. The presence of these peaks means that xylose (~625 s) and the 480 s component are not in perfect phase opposition [18].

The appearance of a new strong correlation between 610 and 633 s in the asynchronous matrix can be related to the existence of new components in the overliming process that interfere. Furthermore the examination of the asynchronous profiles shows the presence of new peaks at ~610 and 633 s (Fig. 6C–F). The signs of the correlation between xylose (~625 s) and the component eluted at 580 s in both synchronous and asynchronous matrix suggest that variations caused by the overliming process start and stop at different times for the two constituents. Modifications in the 580 s peak may appear earlier under mild overliming conditions while the concentration of xylose is still fairly constant (pH 10, 25 °C for 15 and 30 min) (Fig. 3B).

4.3.3. HPLC-UV/HPLC-RI

4.3.3.1. Synchronous matrix. The synchronous matrix resulting from the hetero-2DCOS between the HPLC-RI and HPLC-UV chromatograms is presented in Fig. 4E. While calculating the hetero-correlation matrix, the chromatograms HPLC-UV are considered as *x*-axis. Those related to HPLC-RI are considered as *y*-axis.

A positive peak shows correlation between xylose (625 s) and FF (250 s) (Fig. 7A–D). There are two other negative peaks – one between xylose (625 s) and the group of peaks that appear between 103 and 111 s, the other between FF (250 s) and the 580 s peak. Therefore correlation exists between the peaks of different origin HPLC-RI and HPLC-UV, this deduction will help to highlight variation of reactions or interactions involved during the overliming process.

4.3.3.2. Asynchronous matrix. The examination of the corresponding asynchronous matrix, (Fig. 4F), highlights the presence of peaks in

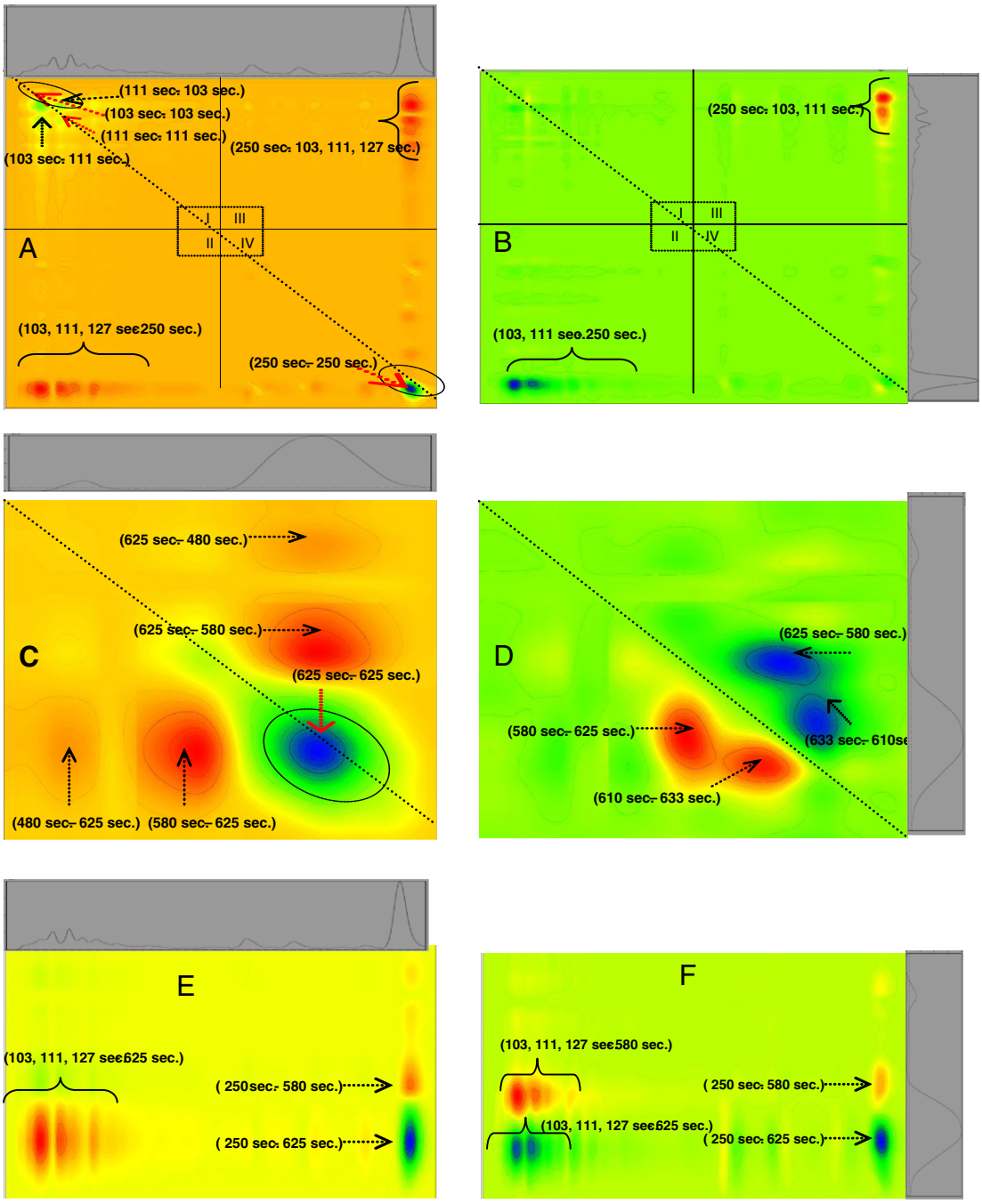

Fig. 4. Matrix resulting from the correlation of: HPLC-UV chromatograms with themselves, (A) Synchronous, (B) Asynchronous; HPLC-RI chromatograms with themselves; (C) Synchronous, (D) Asynchronous; hetero-correlation between the HPLC-RI and HPLC-UV; (D) Synchronous, (E) Asynchronous.

the same places as in the synchronous matrix. This observation can be explained by the fact that carbohydrates (xylose) and furans (FF and HMF) are not the only products present in olive stones DAH [9].

In order to clarify the nature of the changes occurring during the overliming reaction, the retention times and signs of the cross-peaks are listed in Table 2, with the order of events. The presence of positive peaks (250 s–625 s) in the synchronous and asynchronous matrix between xylose (650 s) and furfural (250 s) was expected, this latter being a breakdown product of the former in acidic conditions [9, 15]. However the positive sign in synchronous and asynchronous matrix indicate that FF varies before xylose according to overliming treatments. Examination of Table 1 shows that at pH 10, 25 °C and for 60 min of treatments, FF initial concentration decreases by half while xylose concentration remains constant.

The peak at (103, 111 s–625 s) presents a negative sign in the synchronous matrix but a positive one in the asynchronous matrix; which means that xylose (625 s) starts to vary before the group of peaks appearing towards 103 and 111 s, as a function of the severity of overliming treatment (higher pH, temperature and time).

The peak at (250 s–580 s) presents a negative sign in both synchronous and asynchronous matrix; indicating that modifications appear earlier with FF (250 s) than the component eluted at 580 s.

Fig. 7E and F shows that xylose and the 580 s component vary in opposite directions, while Fig. 7G and H shows that FF and the

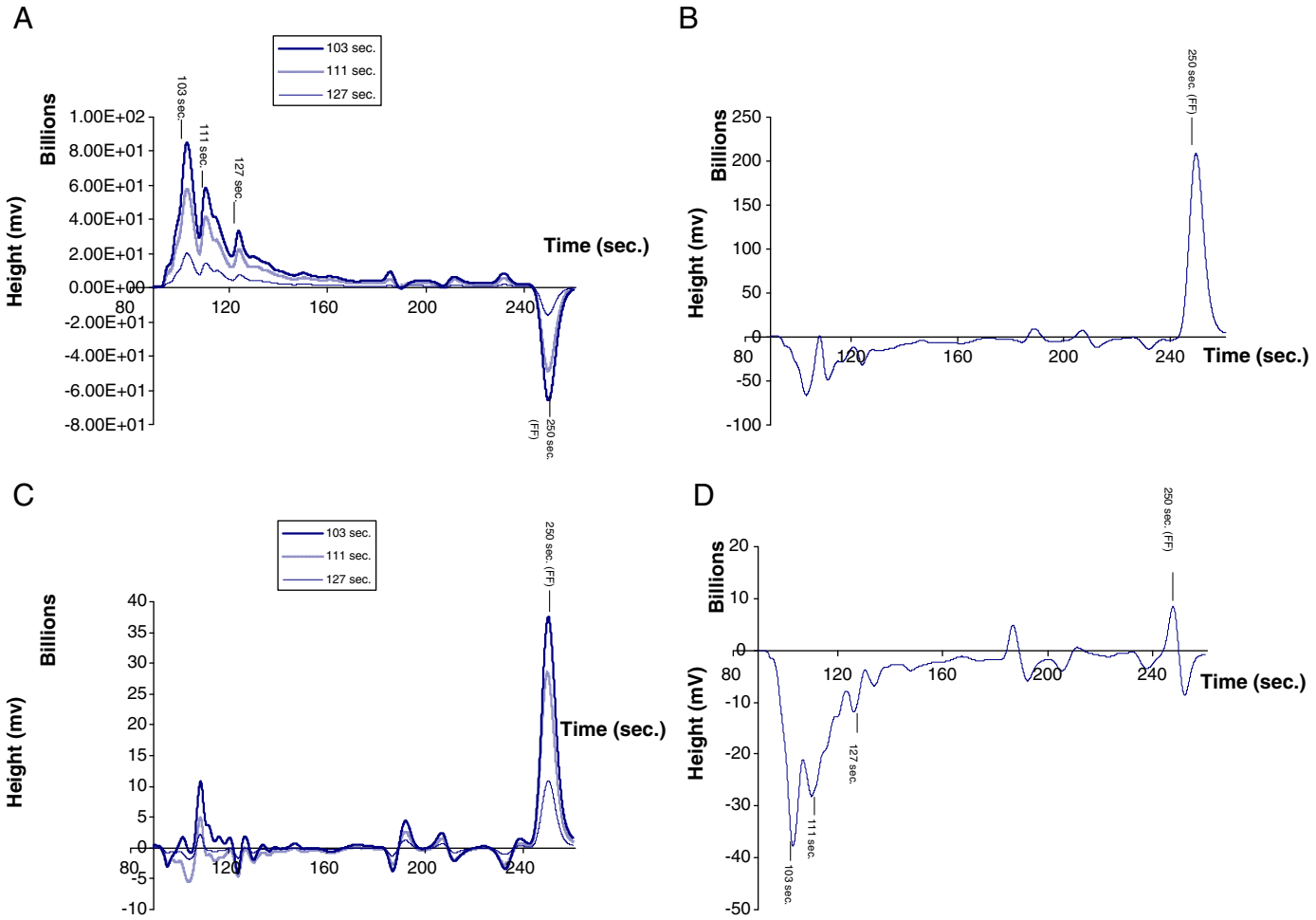

Fig. 5. (A) Synchronous profile HPLC-UV at 103, 111 and 127 s; (B) Synchronous profile HPLC-UV at 250 s, (C) Asynchronous profile HPLC-UV at 103, 111 and 127 s and (D) Asynchronous profile HPLC-UV at 250.

peaks appearing towards 103, 111 and 127 s vary in the same directions, reflecting that a high concentration of FF in DAH leads to more degradation products and vice versa. It was seen that the peak appearing at 127 s presents a weak intensity in the synchronous matrix, while it is almost absent from the asynchronous matrix (Fig. 7A and B).

To complete the study we suggest that during the overliming process the chronological modifications occur first of all for the FF (250 s) then 580 s component, xylose (625 s), and finally for the group of peaks appearing at 103, 111, 127 s When overliming treatments becomes more severe, FF and carbohydrates undergoes degradation and causes an increase in the concentration of components appearing at 103, 111 and 127 s.

Fig. 1A, C and E shows that at pH 10, 25 °C and during the first 15 min of overliming treatment the concentration of xylose, FF and HMF are higher than their concentration in the DAH. This observation can be explained by the preceding deductions concerning the order of appearance of each component during the overliming process. The component appearing at 580 s decreases inducing the increase in xylose concentration, later on carbohydrates (xylose and other non-quantifiable sugars) undergo degradation and enhance the intensity of the group of peaks appearing at 103, 111, 127 s These observations could be of great importance in a kinetic study making it possible to know the order of appearance of these products. It seems that elevation in FF concentration occurs under mild overliming conditions before it degradation with overliming severity. This deduction can be explained by the matrix complexity and the possibility that other components of the DAH interfere with furans degradation.

New peaks appear only in the asynchronous matrix (580 s–110 s) connecting the 580 s compound with the group of peaks appearing at 103, 111, 127 s). The absence of this peak in the synchronous matrix is a sign that these two components are in perfect dephasing and therefore have very distinct behaviours (Fig. 7G and H).

It's well known that in acidic conditions hemi-cellulose is degraded to xylose, mannose, acetic acid and galactose; cellulose is degraded to glucose [9]. Xylose is further degraded to FF and glucose to HMF. Levulinic acid is formed by HMF degradation [34]. Formic acid is released when FF and HMF are broken down [34]. In the same acidic conditions, phenolic compounds are generated from the partial breakdown of lignin [10, 35, 36]. However alkaline degradation of sugar resulted in a complex mixture of more than 50 compounds, including glycolic, lactic, glyceric, 2-C-methylglyceric, deoxytetronic, and deoxypentonic acids [33]. Therefore formic, acetic and lactic acid are eluted at 103 s and 111 s respectively (acetic and lactic acids are not separated). According to Palmqvist et al., another explanation can be proposed: furan derivatives and phenolic compounds react further to form polymeric material [9]. The mechanism of overliming detoxification of DAH is until now unclear. Ageblevor et al. used ^{13}C NMR spectroscopy to elucidate the functional groups involved in the overliming reaction. The ^{13}C NMR spectra show that the major functional groups removed during the overliming process were aliphatic and aromatic acids or esters, and other aromatic and aliphatic compounds. Ketone and aldehyde functions were not

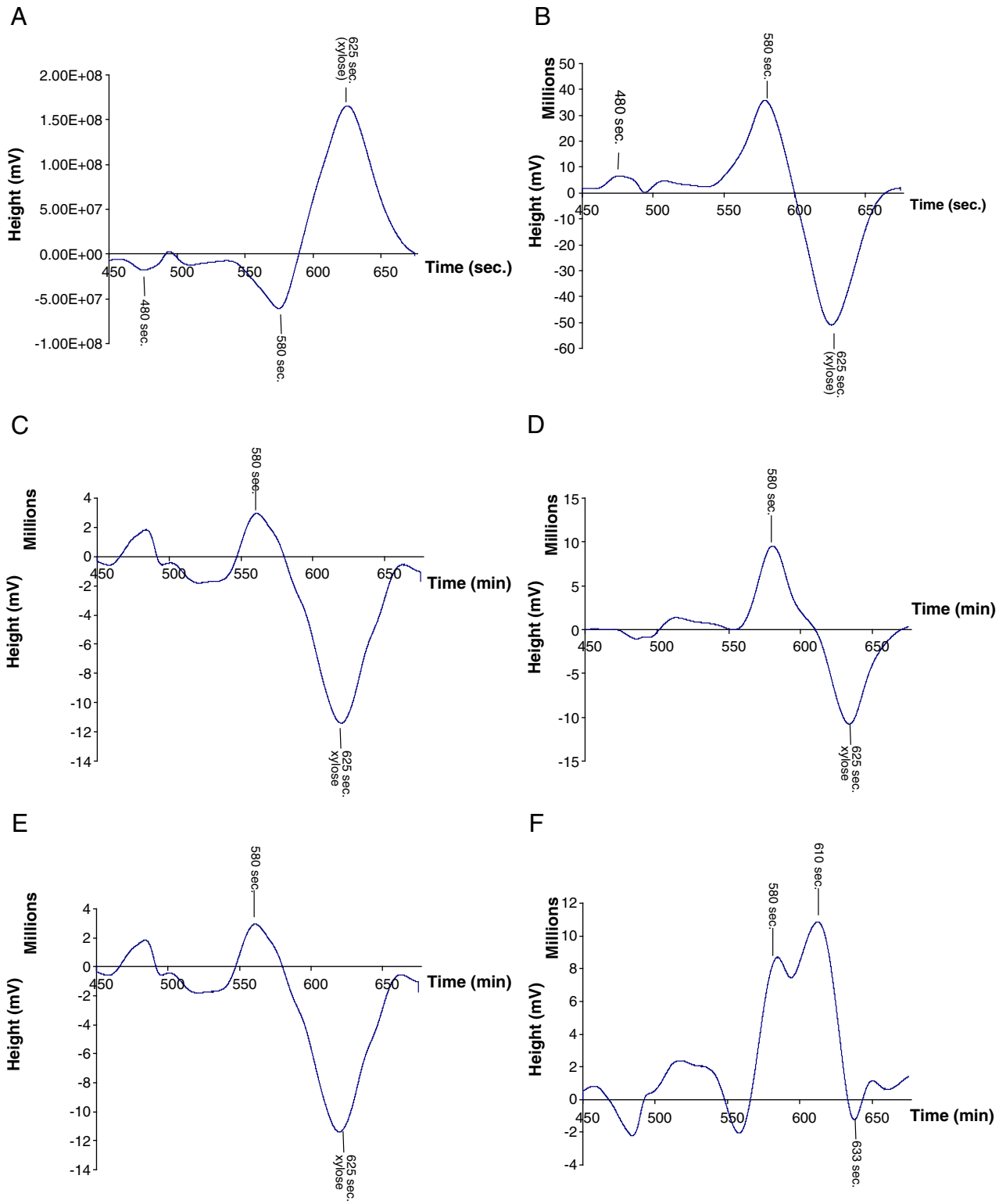

Fig. 6. (A) Synchronous profile HPLC-UV at 580 s; (B) Synchronous profile HPLC-UV at 625 s (C) Asynchronous profile HPLC-UV at 580 s; (D) Asynchronous profile HPLC-UV at 610 s; (E) Asynchronous profile HPLC-UV at 625 s and (F) Asynchronous profile HPLC-UV at 633 s.

detected in the spectra [36]. Palmqvist et al. [9, 14] suggested that the exothermicity of lime hydration (when $Ca(OH)_2$ is added) and the heating of the hydrolysate during the overliming process to reach a higher temperature (60 °C) decreases the solubility of gypsum (formed by divalent calcium from the lime combining with sulfate in the hydrolysate [16]) and so leads to stripping off of volatile compounds such as furfural [37].

In order to reveal the nature of peaks appearing at 103, 111 and 127 s, the diethyl ether extracts of the hydrolysate and the 12 overliming experiments were analysed by gas chromatography/mass spectrometry. Profiles related to the different chromatograms show low molecular weight acids such as acetic and formic acid. These results are concordant with the study of D-fructose reaction under high temperature and pressure which can lead to lactic acid, 1,2,4-

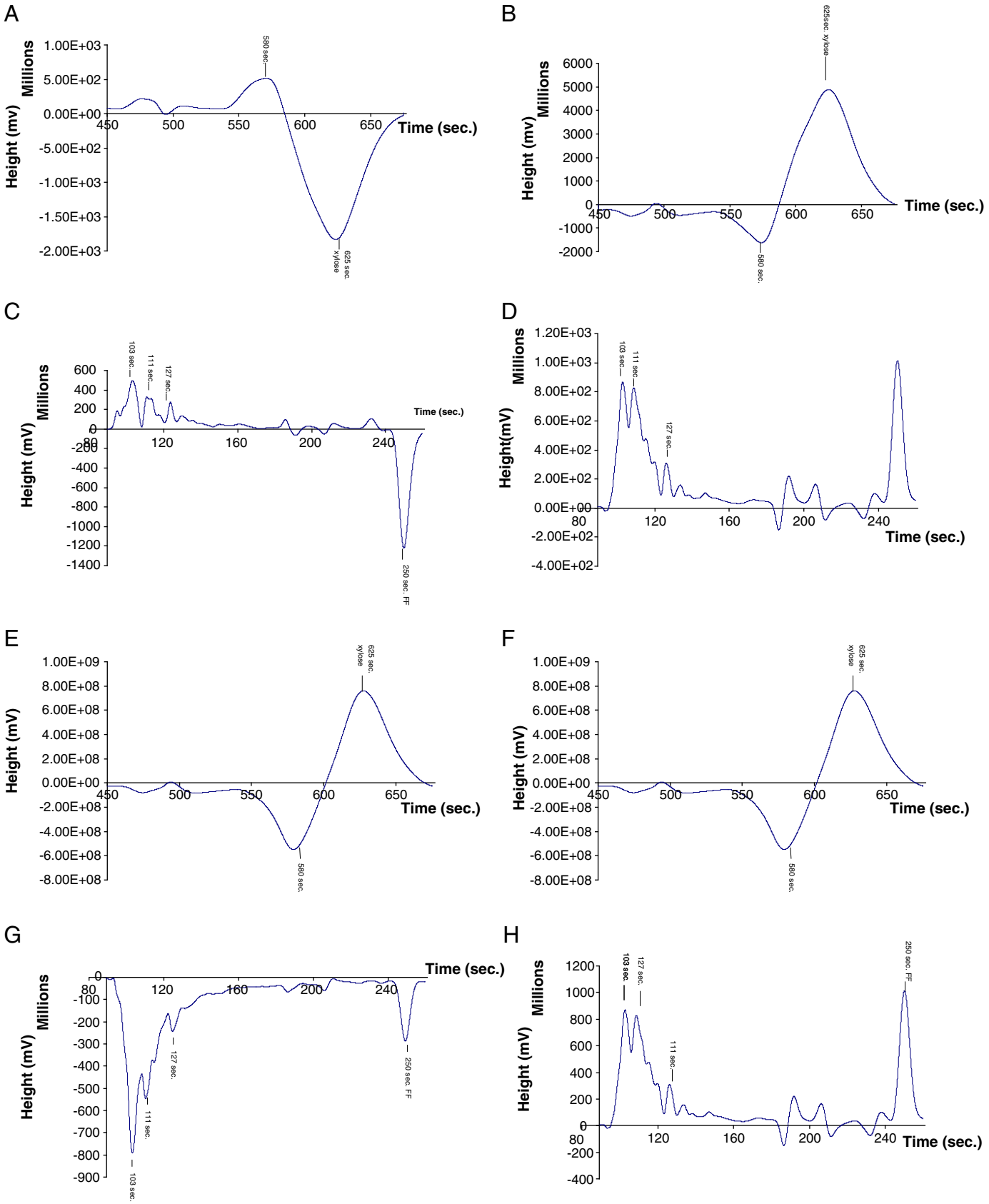

Fig. 7. (A) Synchronous profile HPLC-UV at 103 s; (B) Synchronous profile HPLC-UV at 250 sec; (C) Synchronous profile HPLC-RI at 580 s; (D) Synchronous profile HPLC-RI at 625 s; (E) Asynchronous profile HPLC-UV at 250 s; (F) Synchronous profile HPLC-UV at 103 s; (G) Asynchronous profile HPLC-RI at 580 s and (H) Asynchronous profile HPLC-RI at 625 s.

benzentriol, levulinic and formic acid [32]. This analysis will be completed by an LC-MS for the identification of all products in aqueous solution.

5. Conclusion

The overliming process has been reported as an effective method of reducing toxicity of various hydrolysates such as: yellow poplar, bagasse and spruce [38]. A major drawback of overliming is the sugar loss which was recently reported [39]. Millati [18] added knowledge to this field by reporting the effect of detoxification pH, temperature and duration on the inhibitors and the sugar loss in spruce hydrolysate.

The benefits of the 2DCOS method are that small features that may be overlooked when visually examining complex data sets can be more easily visualised. Moreover, 2DCOS gives important information about the relations that exist among chromatograms. The order in which the constituents vary can be deduced from the sign of peaks in the synchronous and asynchronous matrices, facilitating the interpretation of kinetic studies. In this study we have shown that FF varies before the 580 s component (probably a carbohydrate with four carbons) which, varies before xylose. While xylose undergoes degradation to increase the peaks at 103, 111 and 127 s (sugar degradation products eluted at the beginning of HPLC-UV chromatograms). The presence of other peaks in the synchronous and asynchronous matrices indicates that components other than furans and xylose are also to be found in the DAH and are involved in the overliming process.

Acknowledgement

The authors would like to thank the Lebanese CNRS (Centre Nationale de Recherche Scientifique Libanais) for their financial support.

References

[1] I. Romero, S. Sanchez, M. Moya, E. Castro, E. Ruiz, V. Bravo, Fermentation of olive tree pruning acid-hydrolysates by *Pachysolen tannophilus*, Biochemical Engineering Journal 36 (2007) 108–115.
[2] R. Tengerdy, G. Szakacs, Bioconversion of lignocellulose in solid substrate fermentation, Biochemical Engineering Journal 13 (2003) 169–179.
[3] D. Nabarlatz, A. Ebringerova, D. Montane, Autohydrolysis of agricultural by-products for the production of xylo-oligosaccharides, Carbohydrate Polymers 69 (2006) 20–28.
[4] A. Nefzaoui, Utilisation de la pulpe d'olive comme aliment de sauvegarde, Monastir Tunisie, 1981.
[5] A. Nefzaoui, Etude de l'utilisation des sous-produits de l'olivier en alimentation animale en Tunisie, FAO, Tunisie, 1983.
[6] L'olivier et autres plantes oléagineuses cultivées en Tunisie. Mise au point sur les expériences réalisées sur l'utilisation des grignons d'olive en alimentation animale, Tunisie, 1978.
[7] Tropical Animal Production for the Benefit of man, Valorisation de la pulpe d'olive dans l'alimentation des ruminants, 1982.
[8] S. Medawar, N. Ouaini, R. Daoud, H. Chebib, D. Rutledge, N. Estephan, M. Ismaiili-Alaoui, Etat actuel de l'oléoculture au Liban, New Medit 4 (2005) 53–56.
[9] E. Palmqvist, B. Hahn-Hagerdal, Fermentation of lignocellulosic hydrolysates.II inhibitors and mechanism of inhibition, Bioresource Technology 74 (2000) 25–33.
[10] S. Mussatto, I.C. Roberto, Alternatives for detoxification of diluted-acid lignocellulosic hydrolyzates for use in fermentative processes: a review, Bioresource Technology 93 (2004) 1–10.
[11] S. Larsson, A. Reimann, N. Nilvebrant, J. Jonsson, Comparison of different methods for the detoxification of lignocellulose hydrolyzates of spruce, Applied Biochemistry and Biotechnology 77–79 (1999) 91–103.
[12] Y.H. Zhang, M. Himmel, J. Mielenz, Outlook for cellulase improvement: Screening and selection strategies, Biotechnology Advances 24 (2006) 452–481.
[13] M. Taherzadeh, Ethanol from lignocellulose: physiological effects of inhibitors and fermentation strategies, Biomass and Bioenergy 10 (1999) 367–375.
[14] E. Palmqvist, B. Hahn-Hagerdal, Fermentation of lignocellulosic hydrolysates. I: inhibition and detoxification, Bioresource Technology 74 (2000) 17–24.
[15] J. Maalouly, J. Andary, J. Saab, D. Rutledge, N. Ouaini, Effects of overliming on olive stones diluted acid hyrolysis, Euro FOOD CHEM XIV, (Ed.). Paris, France, 2007, pp. 220–223.
[16] A. Mohagheghi, M. Ruth, D.J. Schell, Conditioning hemicellulose hydrolysates for fermentation: effects of overliming pH on sugar and ethanol yields, Process Biochemistry 41 (2006) 1806–1811.
[17] I. Noda, Advances in two-dimensional correlation spectroscopy, Vibrational Spectroscopy 36 (2004) 143–165.
[18] R. Millati, C. Niklasson, M.J. Taherzadeh, Effect of pH, time and temperature of overliming on detoxification of dilute-acid hydrolyzates for fermentation by *Saccharomyces cerevisiae*, Process Biochemistry 38 (2002) 515–522.
[19] G. Lewis, D. Mathieu, R. Phan-Tan-Luu, Pharmaceutical Experimental Design, (Ed.), Marcel Dekker Inc, N-Y, 1999.
[20] Y. Ozaki, B. Czarnik-Matusewicz, S. Sasic, Two-dimensional correlation spectroscopy in analytical chemistry, Analytical Sciences 17 (2001).
[21] K. Izawa, T. Ogasawra, H. Masuda, H. Okabayashi, I. Noda, Two-dimensional correlation gel permeation chromatography (2D correlation GPC) study of the sol–gel polymerisation of octyltrietoxysilane. HCl-concentration dependance, PhysChemComm 5 (2002) 12–16.
[22] I. Noda, Progress in two-dimensional (2D) correlation spectroscopy, Molecular Structure 799 (2006) 2–15.
[23] P. Harrington, A. Urbas, P. Tandler, Two-dimensional correlation analysis, Chemometrics and Intelligent Laboratory Systems 50 (2000) 149–174.
[24] I. Noda, Kernel analysis for two-dimensional (2D) correlation spectroscopy, Journal of Molecular Structure 799 (2006) 34–40.
[25] Y. Liu, Y. Ozaki, Two-dimensional fourier-transform near-infrared correlation spectroscopy study of dissociation of hydrogen-bonded N-methylacetamide in the pure liquid state, Journal of Physical Chemistry 100 (1996) 7326–7332.
[26] I. Noda, A.E. Dowrey, C. Marcott, Recent developments in two-dimensional infrared (2D IR) correlation spectroscopy, Applied Spectroscopy 47 (1993) 1317–1323.
[27] A.S. Barros, Thesis, INA P-G, Paris, France, 1999.
[28] B. Jaillais, R. Pinto, A.S. Barros, D.N. Rutledge, Outer-Product Analysis (OPA) using PCA to study the influence of temperature on NIR spectra of water, Vibrational Spectroscopy 39 (2005) 50–58.
[29] B. Jaillais, M.-A. Ottenhof, I. Farhat, D.N. Rutledge, Outer-product analysis (OPA) using PLS regression to study the retrogradation of starch, Vibrational Spectroscopy 40 (2006) 10–19.
[30] C. Knill, J. Kennedy, Degradation of cellulose under alkaline conditions, Carbohydrate Polymers 51 (2003) 281–300.
[31] I. Simkovic, J. Alfoldi, M. Matulova, A ^{13}C-N.M.R. study of the alkaline degradation products of polysaccharides, Carbohydrate Research 152 (1986) 137–141.
[32] T. Aida, Y. Sato, M. Watanabe, K. Tajima, T. Nonaka, H. Hattori, K. Arai, Dehydration of D-glucose in high temperature water at pressures up to 80 MPa, Journal of Supercritical Fluids 40 (2007) 381–388.
[33] B.Y. Yang, R. Montgomery, Alkaline degradation of glucose: effect of initial concentration of reactants, Carbohydrate Research 280 (1996) 27–45.
[34] R. Ulbricht, J. Sharon, J. Thomas, A review of 5-hydroxymethylfurfural HMF in parenteral solutions, Fundamental and Applied Toxicology 4 (1984) 843–853.
[35] A. Dupont, C. Egasse, A. Morin, F. Vasseur, Comprehensive characterization of cellulose- and lignocellulose-degradation products in aged papers: capillary zone electrophoresis of low-molar mass organic acids, carbohydrates and aromatic lignin derivatives, Carbohydrate Polymers 68 (2007) 1–16.
[36] F. Agblevor, J. Fu, B. Hames, J. McMillan, Identification of microbial inhibitory functional groups in corn stover hydrolysate by carbon-13 nuclear magnetic resonance spectroscopy, Applied Biochemistry and Biotechnology 119 (2004) 97–120.
[37] L. Olsson, B. Hahn-Hagerdal, Fermentation of lignocellulosic hydrolysates for ethanol production, Enzyme and Microbial Technology 18 (1996) 312–331.
[38] T. Ranatungua, J. Jervis, R. Helm, D. Mcmillan, R. Wooley, The effect of overliming on the toxicity of dilute acid pretreated lignocelulosics: the role of organics, uroic acids and ether-soluble organics, Enzyme and Microbial Technology 27 (2000) 240–247.
[39] A. Martinez, M.E. Rodriguez, S.W. York, J.F. Preston, L.O. Ingram, Effects of $Ca(OH)_2$ treatments ("overliming") on the composition and toxicity of bagasse hemicellulose hydrolysates, Biotechnology and Bioengineering 69 (2000) 526–536.